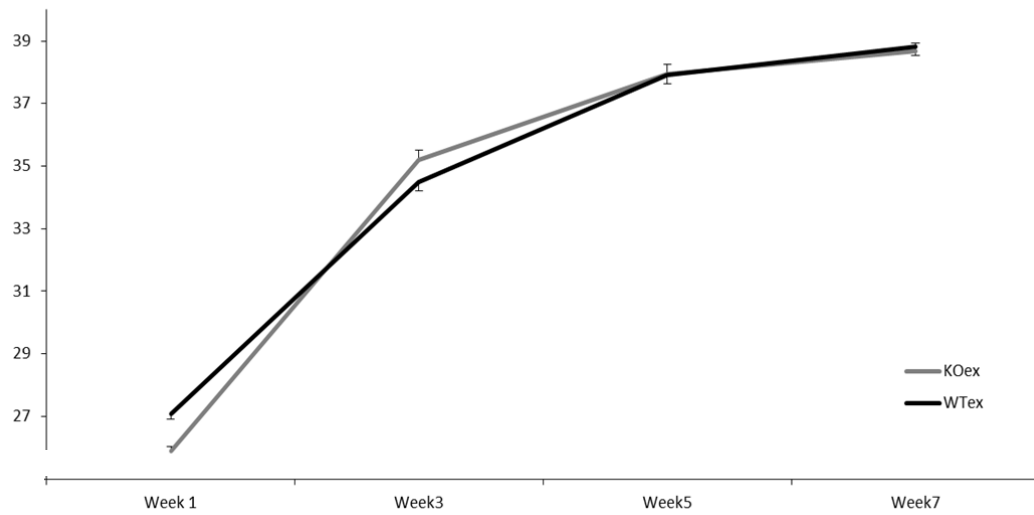


1 **Supplementary Information**

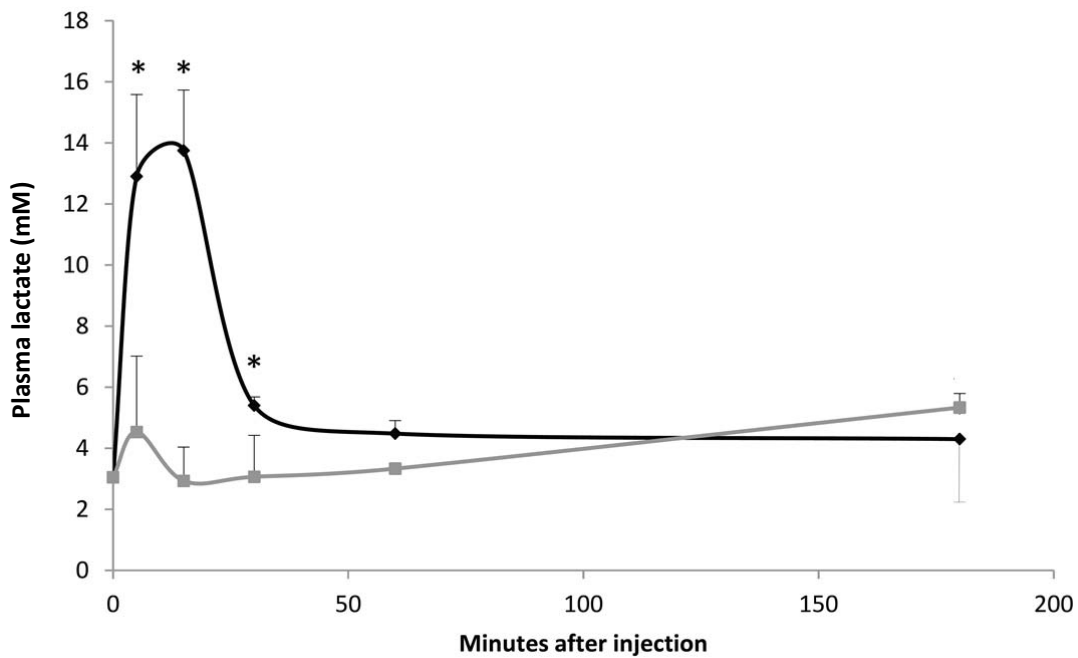
2



3

4 **Supplementary Figure 1 | Physical performance in maximum test.** The maximum running speed of
5 the mice (m/min) in the maximal exercise capacity test (MECT) was not affected by the genotype. It
6 reached a plateau by week 7 of exercise training. The data are presented as mean \pm s.e.m., n = 20
7 mice for KO (8M/12F), n = 21 mice for WT (10M/11F).

8



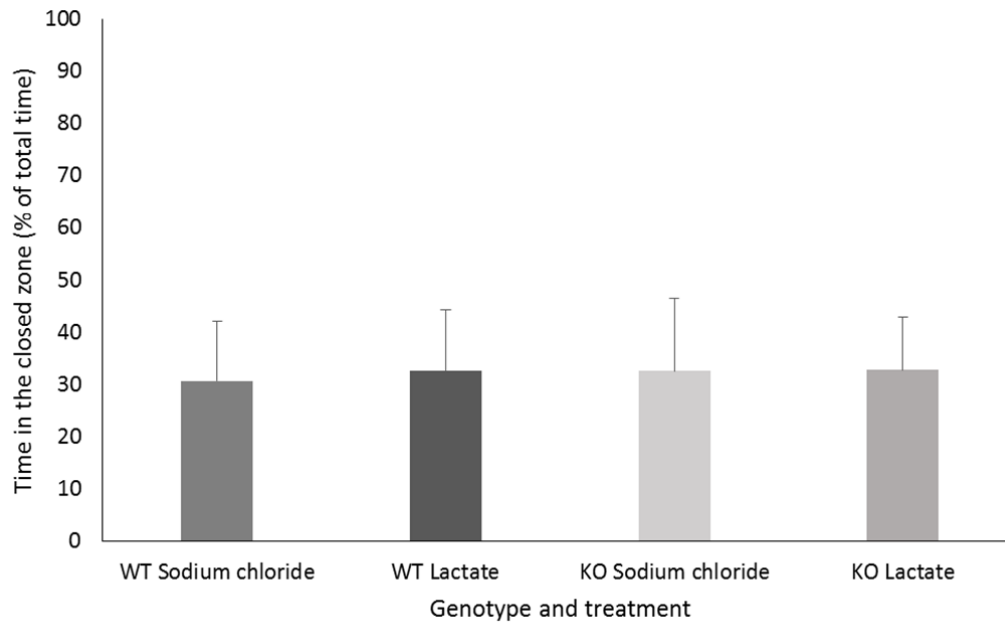
9
10

11

12 **Supplementary Figure 2 | Timecourse of plasma lactate after subcutaneous injection.** Plasma
 13 lactate levels (mmoles/L) increased quickly after a single subcutaneous dose of sodium L-lactate 2.5
 14 g/kg (250 mg/ml, pH 7.4) (black line), but not after injection of the same volume of phosphate
 15 buffered saline (grey line). The lactate concentration peak was between 5 and 15 minutes after the
 16 injection. The data are presented as mean ± s.d., n= 5 mice for each time point for lactate treated
 17 mice and n=3 mice per time point for saline treated mice. The basal lactate concentration (no
 18 injection = "0 minutes") was 3.05 ± 0.72 mM (n = 4). (In this pilot experiment the injected dose was
 19 slightly higher than in the main experiment, 2.0 g/kg.) *, time points at which plasma lactate levels
 20 were significantly higher in mice treated with lactate than in mice treated with the same volume of
 21 saline; $P < 0.05$ (Chi square test; Minitab).

22

23



24

25 **Supplementary Figure 3 | No sign of anxiety attack after lactate injections.** At 15 min after the first
26 injection of lactate, the mice were tested in the elevated zero maze¹. The time spent in the closed
27 zone (a correlate of anxiety) was the same in all experimental groups. Data are presented as mean \pm
28 s.d. of 14-22 mice in each group with a similar gender (M/F) distribution: WT sodium chloride 8M/6F,
29 WT lactate 10M/12F, KO sodium chloride 11M/8F, KO lactate 12M/9F. The frequency of “head-dips”
30 outside the edge of the open zones (negatively correlated with anxiety) was also equal in the groups
31 (not shown). Analysis of variance (ANOVA), $P = 0.96$.

32

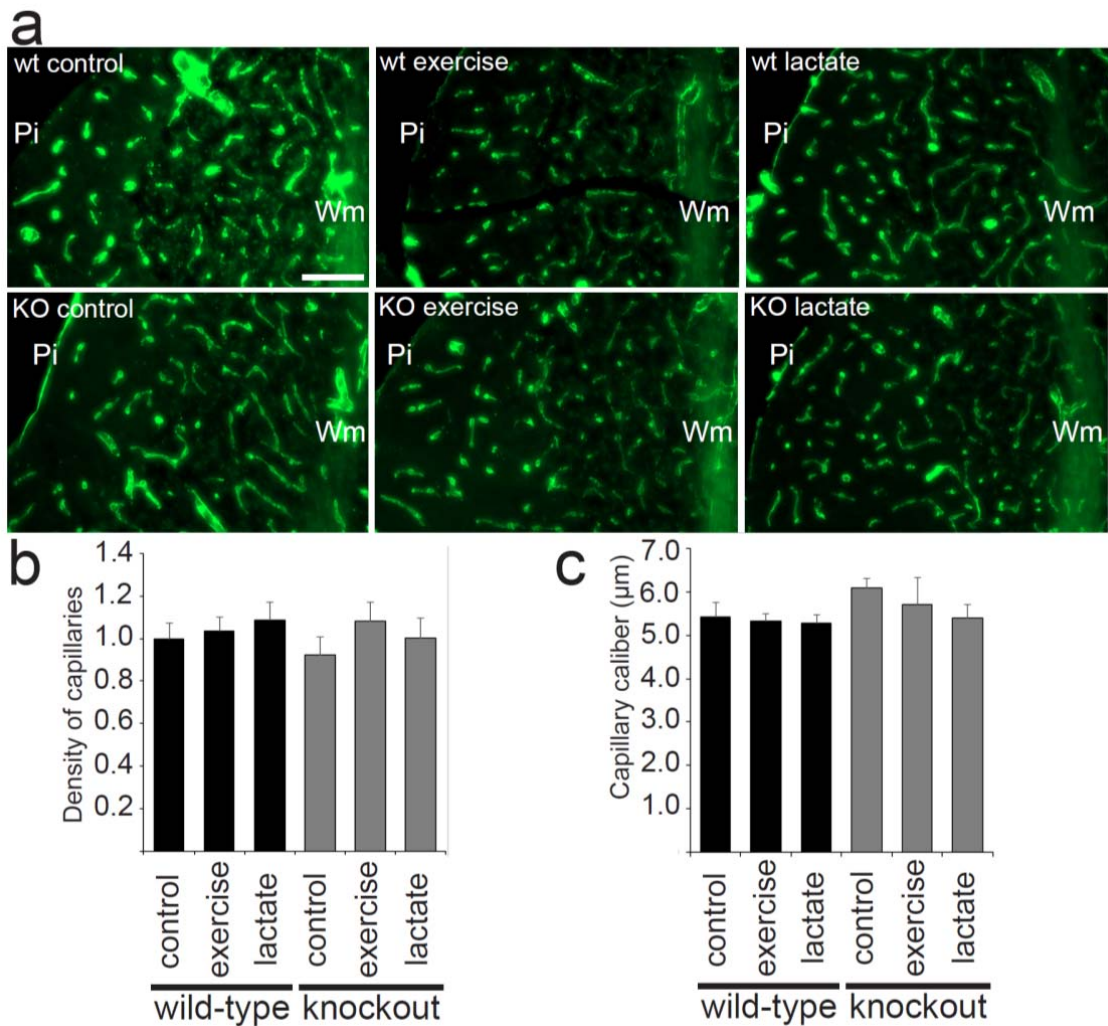
33

34

35

36

37



38

39 **Supplementary Figure 4 | Exercise or lactate cause no change in angiogenesis in the cerebellar**
40 **cortex. a**, Representative images of collagen IV-labelled capillaries in the anterior lobe (folia 1-2) of
41 the cerebellar cortex of wild-type or *Hcar1* knockout mice exposed to vehicle injections (control),
42 treadmill exercise, or lactate injections, 5 days a week for 7 consecutive weeks. Symbols: Pia, pia
43 mater; Wm, white matter. Scale bar: 100 µm. **b**, Quantification of vessel density (in percent of total
44 area, normalized to wild-type control) in the cerebellar cortex. Mean ± s.e.m. of n = 5 wild-type
45 controls, 6 wild-type exercise, 5 wild-type lactate, 5 knockout controls, 4 knockout exercise, and 6
46 knockout lactate mice. ANOVA, $P > 0.05$. **c**, Quantification of vessel diameter in the cerebellar cortex.
47 Mean ± s.d. of the same animals. ANOVA, $P > 0.05$. (Same sections and analysis method as in Fig. 1b.)

48

49

50

51

52

53

54

55

56

57

58

59

60

61

62

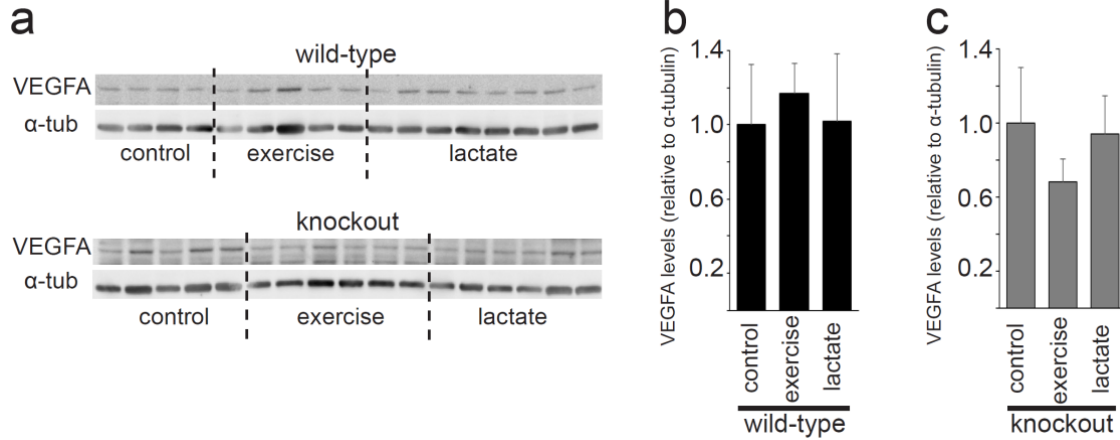
63

64

65

66

67



Supplementary Figure 5 | Exercise or lactate cause no significant change in VEGFA in cerebellum. a,

Images of Western blots underlying analysis in b and c. (Uncropped blots presented in

Supplementary Fig. 6.) **b**, Quantification of VEGFA in cerebellum of wild-type mice. Data are relative to α -tubulin (α -tub), normalized to saline injected wild-type control mice and presented as mean \pm s.e.m. of $n = 4$ wild-type control mice, 5 wild-type exercised mice, and 8 wild-type mice treated with lactate. ANOVA, $P = 0.64$.

c, Quantification of VEGFA in cerebellum of knockout mice. Data are relative to α -tubulin (α -tub), normalized to saline injected knockout control mice and presented as mean \pm s.e.m. of $n = 5$ knockout control mice, 6 knockout exercised mice, and 6 knockout mice treated with lactate. ANOVA, $P = 0.06$.

68

69

70

71

72

73

74

75

76

77

78

79

80

81

82

83

84

85

86

87

88

89

90

91

92

93

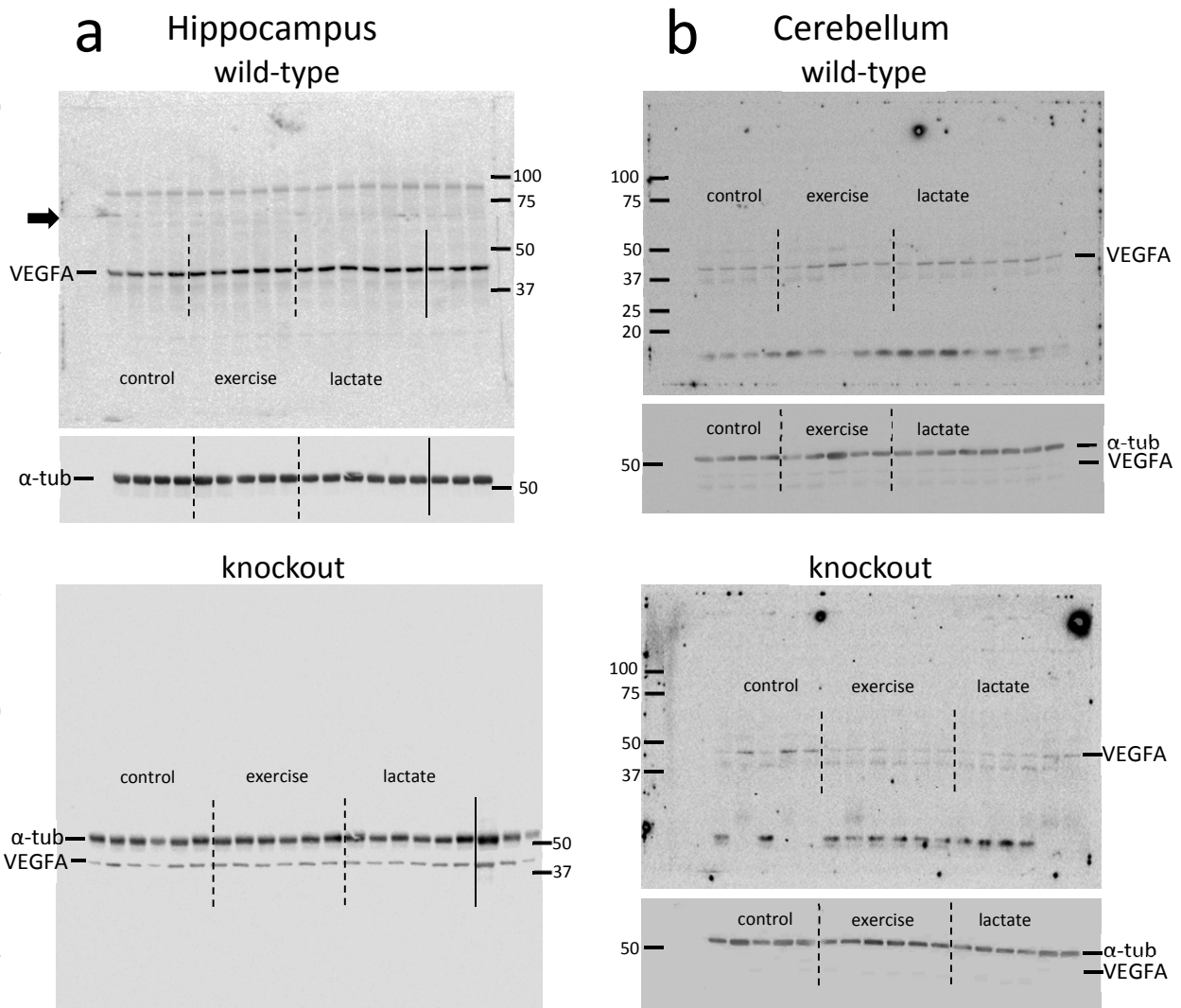
94

95

96

97

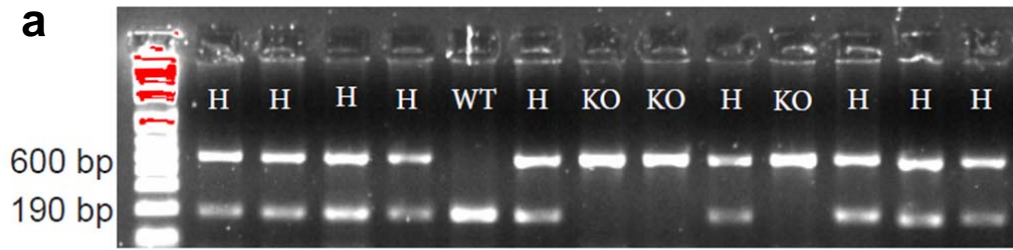
98



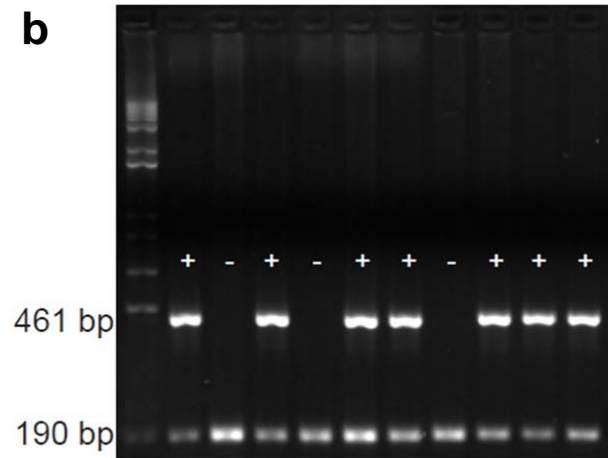
Supplementary Figure 6 | Uncropped scans of Western blots. **a**, Western blots for Fig. 1g, hippocampus. **b**, Western blots for Supplementary Fig. 5a, cerebellum. The membranes were first incubated with VEGFA antibody, then α -tubulin (α -tub) antibody (expected molecular masses VEGFA 43 kDa and α -tub 52 kDa). Among luminescence scans of different exposure times, we selected pictures in which the bands showed suitable intensities for displaying in Fig. 1g and Supplementary Fig. 5a. The scan in a, upper panel, is somewhat over-exposed, serving to show the extent of the membrane. (The upper part of the membrane was cut away, at the fat arrow, to use in an unrelated experiment; it is shown here only for completeness.) The three lanes to the right of the solid vertical lines in a are from heterozygote mice injected with saline (cropped off in Fig. 1g). In cerebellum, the VEGFA antibody showed some extraneous bands that were not seen in hippocampus. The positions of molecular mass markers are indicated, kDa.

99

100



101



102

103 **Supplementary Figure 7 | Transgenic mice, genotypes used.** **a**, *Hcar1* knockout (KO) mice have the
104 190 bp *Hcar1* gene of the wild-type (WT) replaced by the 600 bp *lacZ* gene², both genes are present
105 in heterozygous (H) mice. **b**, mRFP-HCAR1 mice (+) express both *mRFP* (461 bp) and endogenous
106 *Hcar1* (190 bp) under control by the *HCAR1* promoter², wild-type mice (-) only endogenous *Hcar1*.
107 Southern blots.

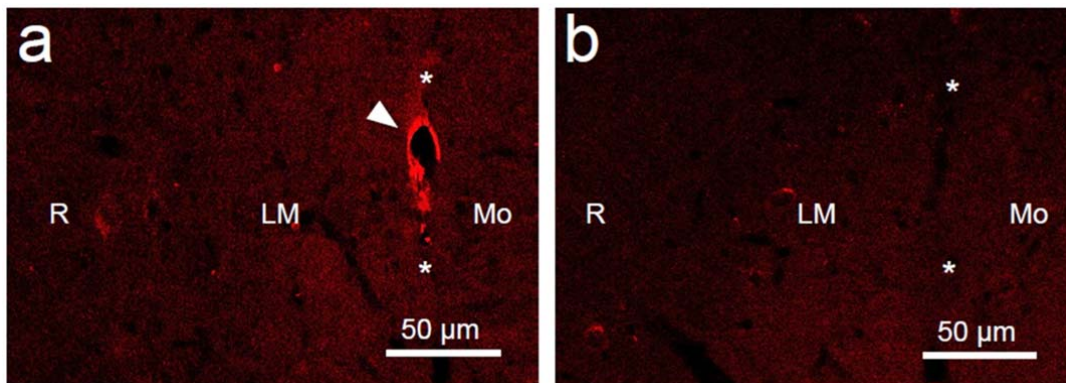
108

109

110

111

112

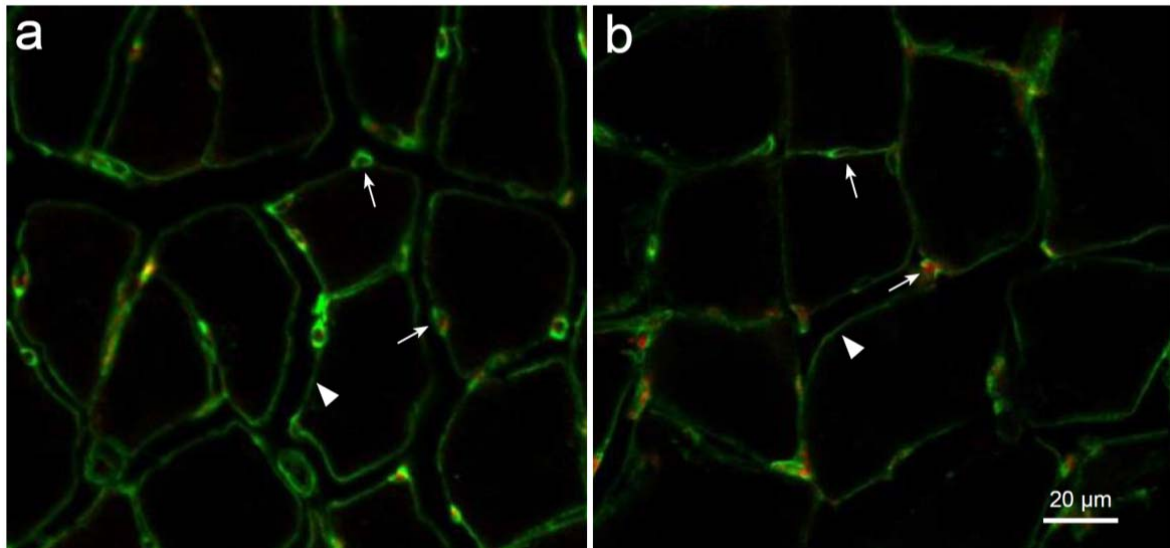


113

114 **Supplementary Figure 8 | Specificity of mRFP immunofluorescence signal. a**, mRFP-HCAR1
115 expressing mouse. **b**, wild-type mouse. Sections were treated with anti-mRFP antibody. Area
116 surrounding fissura hippocampi (asterisks) is shown, with stratum radiatum (R) and stratum
117 lacunosum-moleculare (LM) of hippocampus CA1, and the outer zone of the molecular layer of area
118 dentata (Mo) on opposing sides of the fissure. Arrowhead (**a**) indicates mRFP-HCAR1 expressing pial
119 cells at a blood vessel running in the fissura hippocampi (compare Fig. 3d,i). No mRFP-HCAR1 at
120 vessels in wild-type mouse (**b**).

121

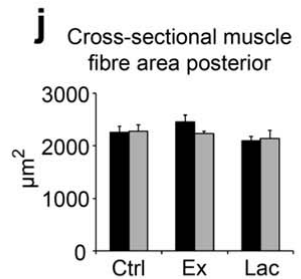
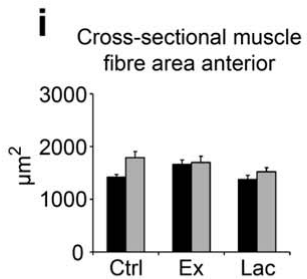
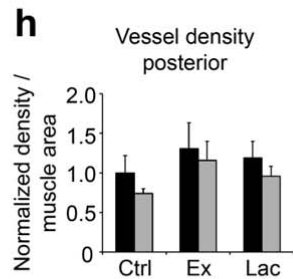
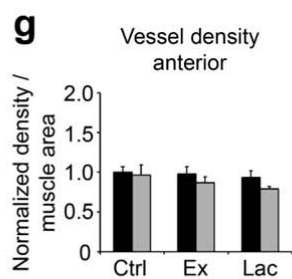
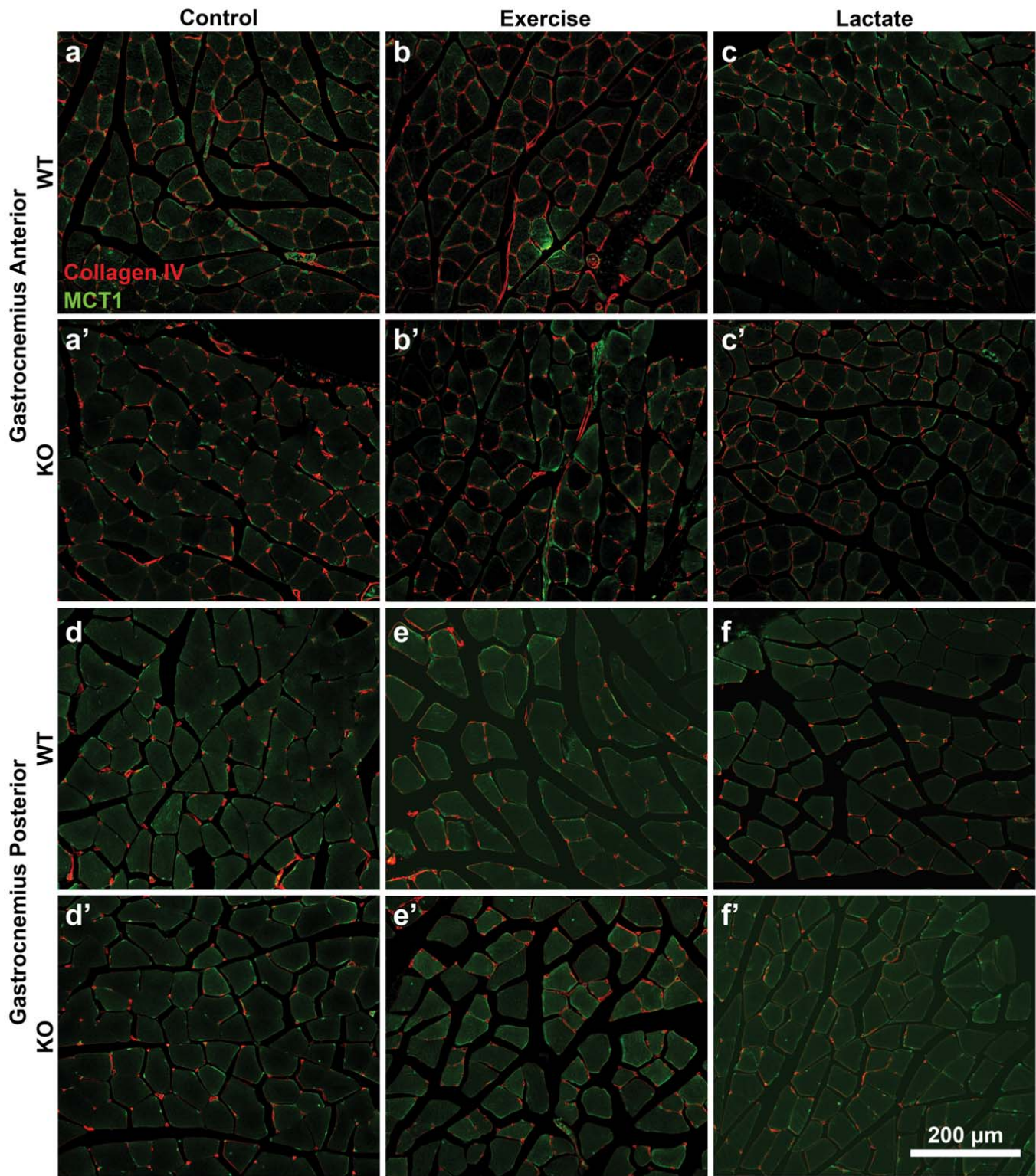
122



123

124 **Supplementary Figure 9 | No significant HCAR1 localization in skeletal muscle.** **a**, mRFP-HCAR1
125 reporter mouse. **b**, wild-type mouse. Soleus part of the triceps surae muscle. Basement membrane
126 in capillaries (arrows) and around muscle fibres (arrowheads) are visualized by immunolabelling for
127 collagen IV (green). No significant mRFP-HCAR1 signal (red); traces of red in some capillaries, in both
128 a and b, represent autofluorescence.

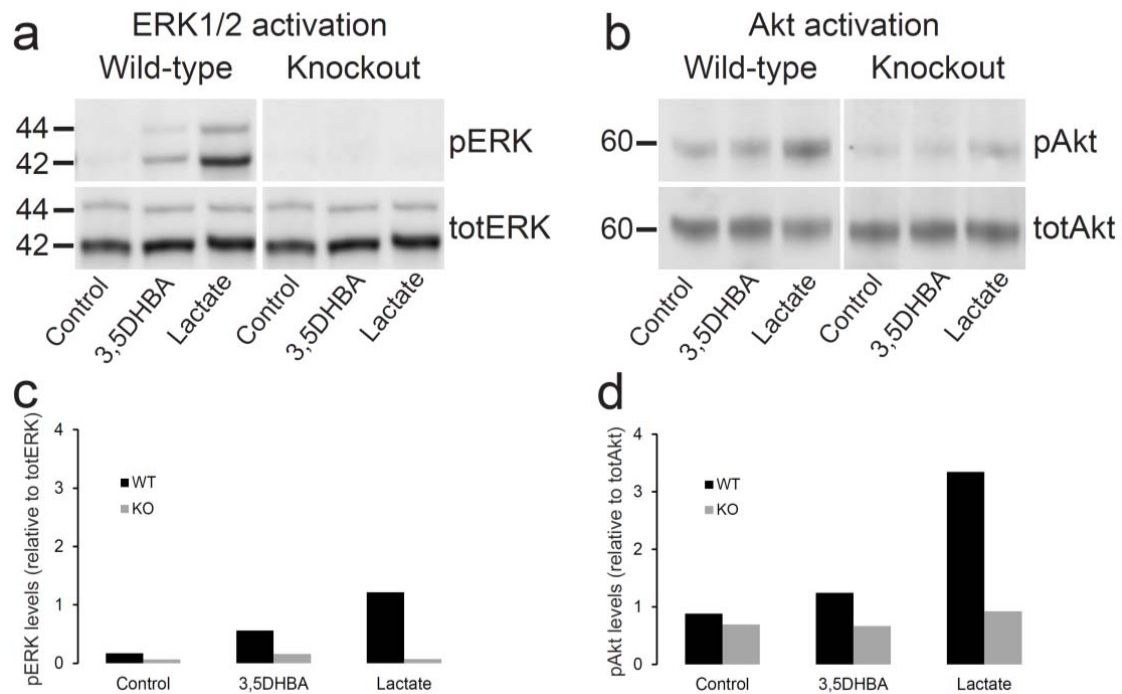
129



■ WT
□ KO

131 **Supplementary Figure 10 | No angiogenic effect of exercise or lactate in skeletal muscle. a-f,**
132 Images of collagen IV-labelled capillaries (red) in the anterior (a-c) and posterior (d-f) gastrocnemius
133 muscle (parts of the triceps surae muscle) of wild-type (a-f) or *Hcar1* knockout (a'-f') mice exposed to
134 vehicle injections (control), treadmill exercise, or lactate injections, 5 days per week for 7
135 consecutive weeks. The sections were co-labelled for monocarboxylate transporter 1 (MCT1, green)
136 to visualize the muscle fibres. **g-h**, Normalized density \pm SEM of collagen IV-labelled capillaries
137 associated with muscle fibres in gastrocnemius anterior (g) and posterior (h). **i-j**, Average cross-
138 sectional area \pm s.e.m. of muscle fibres in gastrocnemius anterior (i) and posterior (j). Ctrl, sedentary
139 vehicle control; Ex, exercise; Lac, lactate. n = 5-6 mice per group. ANOVA showed no significant
140 differences among the results, except in i, but the post hoc test showed significance only between
141 the controls.

142



143

144 **Supplementary Figure 11 | HCAR1 activates ERK1/2 and Akt, which are known to induce**
 145 **angiogenesis through VEGFA³.**

146 **a-b**, Western blots showing HCAR1 stimulation of phosphorylation of ERK1/2 and Akt in mouse
 147 hippocampal slices. **a**, Phosphorylated ERK (pERK; upper panel) in *Hcar1* knockout and wild-type
 148 slices after exposure to Krebs buffer (Control) or Krebs buffer containing the HCAR1 selective agonist
 149 3,5-dihydroxybenzoate (3,5DHBA) 2mM, or sodium L-lactate (Lactate) 10mM, for 90 minutes at 30°C.
 150 Both agonists induced ERK phosphorylation in wild-type mice but not in *Hcar1* knockouts. **b**,
 151 Phosphorylated Akt (pAkt; upper panel) in *Hcar1* knockout and wild-type slices as in **a**. Both agonists
 152 induced Akt phosphorylation in wild-types but not in *Hcar1* knockouts. Total ERK (totERK) and total
 153 Akt (totAkt) signals were largely unaffected by treatment and genotype. **c-d**, Quantification of
 154 Western blots as shown in **a** and **b**, expressed relative to totERK1/2 and totAkt, respectively, used as
 155 loading controls; means of two runs.

156

157 **Supplementary References**

- 158 1. Shepherd JK, Grewal SS, Fletcher A, Bill DJ, Dourish CT. Behavioural and pharmacological
 159 characterisation of the elevated "zero-maze" as an animal model of anxiety.
 160 *Psychopharmacology (Berl)* **116**, 56-64 (1994).
 161
 162 2. Ahmed K, *et al.* An autocrine lactate loop mediates insulin-dependent inhibition of lipolysis
 163 through GPR81. *Cell Metab* **11**, 311-319 (2010).
 164
 165 3. Wang L, *et al.* Neural progenitor cells treated with EPO induce angiogenesis through the
 166 production of VEGF. *J Cereb Blood Flow Metab* **28**, 1361-1368 (2008).

167

168

169

170 **Supplementary Table 1 | *Hcar1* expression in tissues of wild-type and knockout mice**

EXP.#	TISSUE	WILD-TYPE	SEM	n	KNOCKOUT	SEM	n
1	Hippocampus	1	0.52	5	0.00030	0.00015	5
	Liver	0.0046	0.0038	4	0.00024	0.00009	3
	Muscle	0.342	0.093	5	0.00008	0.00004	4
	Fat	75	30	4	0.0013	0.0012	2
2	Hippocampus	1	0.148	4	<0.008	<0.001	5
	Meninges	7.6		5*	0.08		5*

171

172 *Hcar1* mRNA expression is given relative to that of the house-keeping gene, *RPS18r* (Experiment #1),
173 or *Rpl27a* (Experiment #2), and normalized to the value for hippocampus (= 1). SYBR-green
174 (Experiment #1) or TaqMan based detection (Experiment #2) was used.

175 *, Meninges from 5 mice were pooled to get enough material for analysis.

176

177

178 **Supplementary Table 2 | Capillary area fraction and volume fraction in sensorimotor cortex**

	wt vehicle	wt exercise	wt lactate	ko vehicle	ko exercise	ko lactate
AF	8.36±0.49	9.40±0.45	9.99±0.86	8.44±0.31	8.13±0.68	8.31±0.69

179

180 The table shows the area fraction (AF, % of tissue volume, mean ± s.d.) of capillaries in sensorimotor
 181 cortex, i.e., the ‘raw data’ underlying the relative values of capillary density presented for wild-type
 182 (wt) and *Hcar1* knockout (ko) mice in the main Fig. 1b (there as mean ± s.e.m.). The AF was
 183 determined blind by point-counting on images acquired from 20 µm parasagittal sections using an
 184 automated slide scanner system (see Methods). The volume fraction (VF) can be obtained from the
 185 area fraction (AF), the mean capillary diameter (dC), and the section thickness (t), through the
 186 formula $VF = AF \cdot dC / t$ (see Weber, B., Keller, A.L., Reichold, J. & Logothetis, N.K. The microvascular
 187 system of the striate and extrastriate visual cortex of the macaque. *Cereb. Cortex* **18**, 2318-2330
 188 (2008), in its Appendix on stereological computations, p 2328). $AF = 8.4\%$ in wt as well as ko controls
 189 (this Table), $dC = 5.8 \mu\text{m}$ (outer diameter, equal in all the experimental conditions, see legend of
 190 Fig.1), and $t = 20 \mu\text{m}$. Hence $VF = 8.4\% \cdot 5.8 \mu\text{m} / 20 \mu\text{m} = 2.4\%$. Thus capillaries occupy 2.4% of the
 191 volume of cortex gray matter in the control condition. (Note that the conversion factors do not
 192 change among the experimental conditions, and that conversion to ‘absolute’ VF values is not
 193 required for determining the relative changes in capillary density caused by exercise and lactate,
 194 displayed in Fig. 1b.)

195